Yasuo Satô *

Propagation of Torsional Disturbances in a Homogeneous Elastic Sphere

Abstract: Localized torsional stress is applied on the surface of a homogeneous elastic sphere for a short duration of time. The propagation of the disturbance caused by this stress is calculated numerically by superposing the normal mode solutions. The phases of the body waves and surface waves are obtained.

Symbols

a	radius of the sphere
r, θ, φ	radial distance, colatitudinal angle and azimuthal angle
u, v, w	radial, colatitudinal and azimuthal components of the displacement
$f(t), \Phi(\theta, \varphi)$	time and space distributions of the source function
i, n	mode number and order of harmonics
p	frequency
V_P, V_S	velocity of P and S waves
k	$= p/V_S$
J_n	Bessel function
λ, μ	Lamé constants

1. Introduction

A basic problem in the field of theoretical seismology is to prescribe a localized stress within or on the surface of an elastic medium and to determine the propagation of disturbances transmitted from this source. Such a problem for a half-space bounded by a plane, free surface is an historically famous one, which was solved by H. Lamb[1] in 1904. Since then many similar papers have been published, most of them being concerned with the case of one or more parallel plane boundaries.

In this paper, a localized shear stress on the surface of a homogeneous elastic sphere is prescribed. If a similar kind of stress is prescribed in a region with plane boundaries, the surface waves may be viewed as the contribution from the poles of an integral representation of the solution, while the body waves may be represented as the contribution from the branch points. In our present problem, however, the integral representation of the solution does not have any branch points. Consequently, all the disturbances satisfying the boundary conditions are superpositions of normal mode solutions. Thus the displacements of points on the surface are obtained by calculation of the residues. The ray paths and notations for the various waves are shown in Fig. 1. Subsequent Figures give numerical results for the surface displacements.

2. Propagation of the torsional disturbance

The solution of the equation of motion of a homogeneous

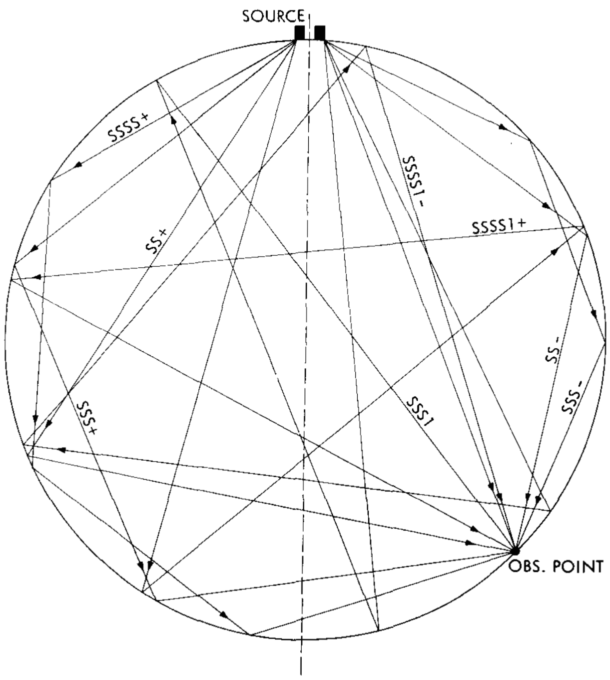

Figure 1 **Ray paths and the notations of various phases of S waves.**

* Present address: Earthquake Research Institute, Tokyo University.

elastic solid is given by

$$\mathfrak{D} = {}_0\mathfrak{D} + {}_1\mathfrak{D} + {}_2\mathfrak{D}$$
$$= \text{grad}\ \Phi + \text{rot}\ (r\cdot{}_1\Psi,\ 0,\ 0)$$
$$+ \text{rot rot}\ (r\cdot{}_2\Psi,\ 0,\ 0),$$

where $\mathfrak{D}$ implies the displacement vector. Φ, ${}_1\Psi$ and ${}_2\Psi$ are the functions satisfying the wave equations

$$\nabla^2\Phi = V_P^{-2}\ \partial^2\Phi/\partial t^2$$
$$\nabla^2{}_i\Psi = V_S^{-2}\ \partial^2{}_i\Psi/\partial t^2 \qquad (i = 1, 2).$$

${}_0\mathfrak{D}$ = grad Φ gives the dilatational wave, ${}_1\mathfrak{D}$ = rot$\cdot$ $(r\cdot{}_1\Psi, 0, 0)$ the rotational wave of the first kind and ${}_2\mathfrak{D}$ = rot rot $(r\cdot{}_2\Psi, 0, 0)$ that of the second kind.

The problem we discuss is as follows: Without employing the dilatational wave, satisfy the boundary conditions

$$\widehat{rr} = \lambda\ \text{div}\ \mathfrak{D} + 2\mu\frac{\partial u}{\partial r}$$
$$\widehat{r\theta} = \mu\left\{r\frac{\partial}{\partial r}\left(\frac{v}{r}\right) + \frac{1}{r}\frac{\partial u}{\partial \theta}\right\}$$
$$\widehat{r\varphi} = \mu\left\{\frac{1}{r\sin\theta}\frac{\partial u}{\partial\varphi} + r\frac{\partial}{\partial r}\left(\frac{w}{r}\right)\right\}$$
$$= \Phi(\theta, \varphi)\cdot f(t) \quad \text{at} \quad r = a. \tag{2.1}$$

This is a special case of Problem S given in our previous study.[3] If we confine attention to axisymmetric boundary data, then

$$\Phi(\theta, \varphi) = \Phi^0(\cos\theta), \tag{2.2}$$

and we have the simplified formulae

$$\widehat{rr} = 0,$$
$$u = 0,$$
$$v = 0,$$
$$w(p) = -\sum_n B_n{}^0\cdot g_n\cdot\frac{d}{d\theta}P_n(\cos\theta), \tag{2.3}$$

where

$$B_n = \xi_n{}^0/E_2$$
$$E_2 = \mu r d(g_n/r)/dr$$
$$\xi_n{}^0 = K_n{}^{0\prime}\int_{-1}^{1}\frac{d}{d\theta}\{\sin\theta\cdot\Phi^0(\cos\theta)\}$$
$$\times (P_n/\sin\theta)d(\cos\theta)$$
$$K_n{}^{0\prime} = (2n+1)/\{2n(n+1)\}$$
$$g_n = (kr)^{-\frac{1}{2}}J_{n+\frac{1}{2}}(kr), \quad k = p/V_S. \tag{2.4}$$

In order to satisfy the boundary condition (2.1), we integrate the expression given in (2.3), namely

$$w = \int_{-\infty}^{\infty} w(p)f^*(p)\exp(jpt)dp, \tag{2.5}$$

where $f^*(p)$ is the Fourier transform of the function $f(t)$, and $j = \sqrt{-1}$.

Since there are no branch points in the integrand of (2.5), this integral can be evaluated by contour integration and is given by the expression

$$w = -\sum_n\frac{1}{2\pi}\xi_n{}^0\frac{d}{d\theta}P_n(\cos\theta)\int_{-\infty}^{\infty}(g_n/E_2)f^*(p)$$
$$\times \exp(jpt)dp$$
$$= j\frac{V_S}{2\mu}\left(\frac{a}{r}\right)^{1/2}\sum_n\xi_n{}^0\frac{d}{d\theta}P_n$$
$$\times\sum_i\left[\frac{J_{n+\frac{1}{2}}(kr)}{\frac{3}{2}J_{n+\frac{1}{2}}(ka)+\{(n-1)(n+\frac{1}{2})(ka)^{-1}-ka\}J_{n+\frac{1}{2}}(ka)}\right.$$
$$\left.\times f^*(p)\exp(jpt)\right]_{p={}_ip_n} \tag{2.6}$$

in which i is the mode number. (When $f^*(p)$ has any poles the residues which come from those singularities should be taken care of.) The roots ${}_ip_n$ of the characteristic equation,

$$E_2 = 0, \tag{2.7}$$

were previously obtained by the present authors.[2]

The real part of the above expression is used for the numerical computation.

3. Numerical computation

In carrying out the numerical computation, we put

$$\Phi^0(\cos\theta) = \begin{cases} 1 & \theta_1 < \theta < \theta_2 \\ 0 & \theta < \theta_1, \quad \theta_2 < \theta \end{cases} \tag{3.1}$$

$$f(t) = \begin{cases} 1/(2t_1) & -t_1 < t < t_1 \\ 0 & t < -t_1, \quad t_1 < t. \end{cases} \tag{3.2}$$

For the function of time $f(t)$ given above, we have

$$f^*(p) = (\sin pt_1)/p \tag{3.3}$$

and, in the numerical work, the following values for the parameters in (3.1)-(3.2) were assumed:

$$\theta_1 = 0.02, \qquad \theta_2 = 0.04,$$
$$t_1 = 0.015. \tag{3.4}$$

In the last expression, the unit of time is taken to be $2\pi a/V_S$ = (circumference of the sphere/shear wave velocity).

The azimuthal displacement ${}_iw_n$ on the surface, which is the contribution of the ${}_iT_n$ mode, is computed as a function of time. The total displacement w = $({}_iw_n)$ is obtained by summing the contributions from all the modes up to and including ${}_iT_n$.

The computation was carried out for 300 modes, with $i = 5$ and $n = 60$, i.e., ${}_5w_{60} = \sum_{i=1}^{5}\sum_{n=1}^{60}{}_iw_n$. In Fig. 2, however, we show not only $({}_5w_{60})$ (solid line), but also $({}_1w_{60})$ (broken line) and $({}_1w_{10})$ (chain line). The disturbance for very small values of time is not accurate.

Partial view of oversized sheet

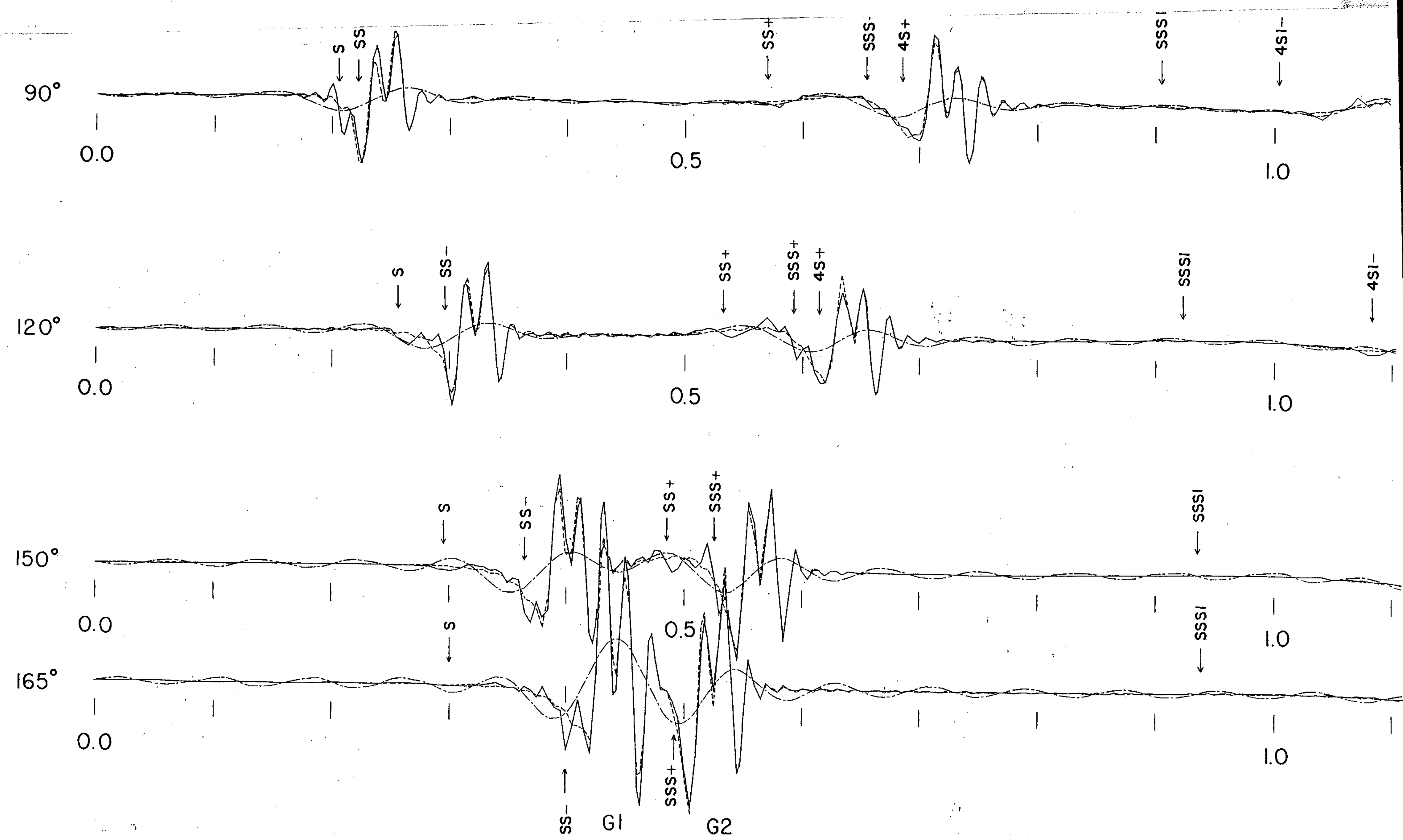

Figure 2 **Azimuthal displacement w caused by a localized shear stress applied on the surface of a homogeneous elastic sphere.**

Unit of time is $(2\pi a/V_S)$.
Solid line ——— $({}_5w_{60})$, *Broken line* - - - $({}_1w_{60})$,
Chain line —·—·— $({}_1w_{10})$.

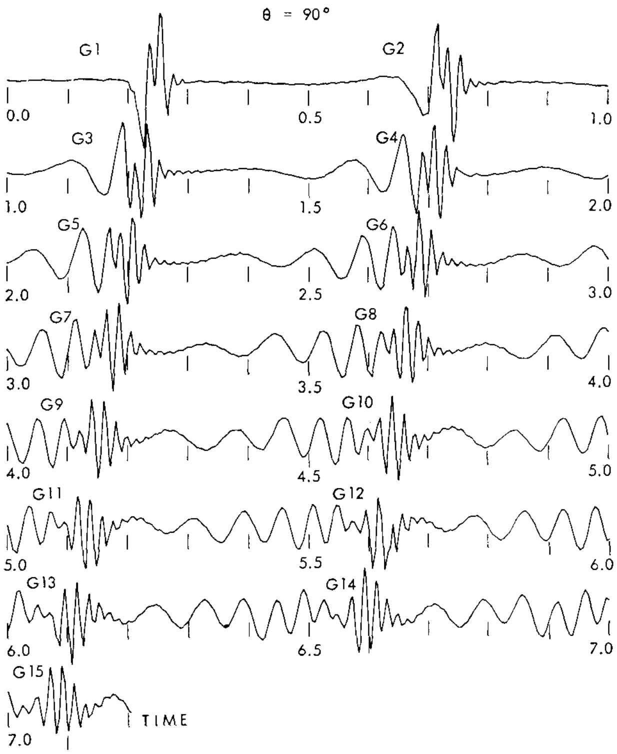

Figure 3 **Azimuthal displacement on the equator ($\Theta = 90°$).**
$w = ({}_1w_{60})$. *Unit of time is* $(2\pi a/V_S)$.

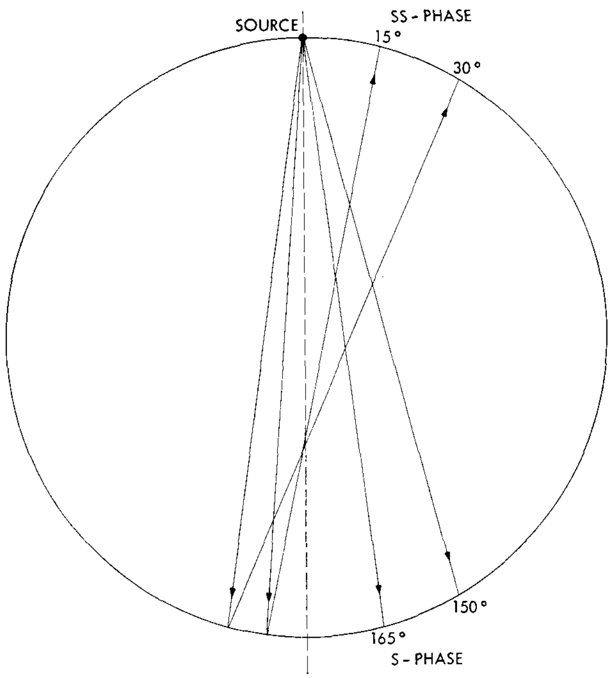

Figure 4 **Ray path of waves passing the very deep part of the spherical medium.**

Arrows show the arrival times of various body waves calculated by means of geometrical optics. The notation nSm denotes the S wave which has reflected $(n - 1)$ times at the surface and which has arrived at a point having epicentral distances $2m\pi + \theta$ or $(2m + 1)\pi - \theta$ after the wave has traveled along the minor $(-)$ or major $(+)$ arc (see Fig. 1). Comparing $({}_1w_{60})$ and $({}_5w_{60})$ in Fig. 2, we notice that the body waves appear more strongly in the latter than in the former. This means that, in general, higher modes of free oscillation give rise mostly to body waves and lower modes to surface waves. This can be also inferred from the Figure in our previous work,[4] which shows that higher modes have a larger amplitude in the interior of a sphere than lower modes. It may also be observed from Fig. 2 that the wave S at $\theta = 150°$, $165°$ and the wave $SS+$ at $15°$, $30°$ can hardly be distinguished. If we draw the rays of these waves which deeply penetrate the sphere, the above observation indicates that our computation, taking into account only the modes ${}_iT_n$ up to $i = 5$, $n = 60$, is not sufficiently accurate to determine the nature of a deep body wave (See Fig. 1).

Within certain limitations, our model for the elastic sphere might be applied to seismological problems. In this respect, it is worth mentioning that, for certain points, the curves $G1$ and $G3$, $G2$ and $G4$ have similar features except for their signs. (See Fig. 3, which is the disturbance for $\theta = 90°$, $w = ({}_1w_{60})$.) This similarity is caused by the polar phase shift discovered by Brune, Nafe, and Alsop.[5] (See Fig. 4.)

Figure 5 is a three-dimensional figure of $({}_1w_{10})$ showing how the wave is propagated on the surface of a sphere.

Acknowledgments

The author acknowledges his indebtedness to Professor W. J. Eckert, who gave him the opportunity to work at the Watson Research Laboratory. All the computations were performed on an IBM 7090.

References

1. H. Lamb, "On the propagation of tremors over the surface of an elastic solid," *Phil. Trans. Roy. Soc. London* **A 203,** 1-42 (1904).
2. Y. Satô and T. Usami, "Basic study on the oscillation of a homogeneous elastic sphere I. Frequency of the free oscillation," *Geophys. Mag.* **31,** 15-24 (1962).
3. Y. Satô and T. Usami, "Basic study on the oscillation of a homogeneous elastic sphere III. Boundary conditions and generation of elastic waves," *Geophys. Mag.* **31,** 49-62 (1962).
4. Y. Satô and T. Usami, "Basic study on the oscillation of a homogeneous elastic sphere II. Surface distribution of displacement," *Geophys. Mag.* **31,** 25-47 (1962).
5. N. N. Brune, J. E. Nafe and L. E. Alsop, "The polar phase shift of surface waves on a sphere," *Bull. Seism. Soc. Amer.* **51,** 247-258 (1961).

Received July 2, 1962

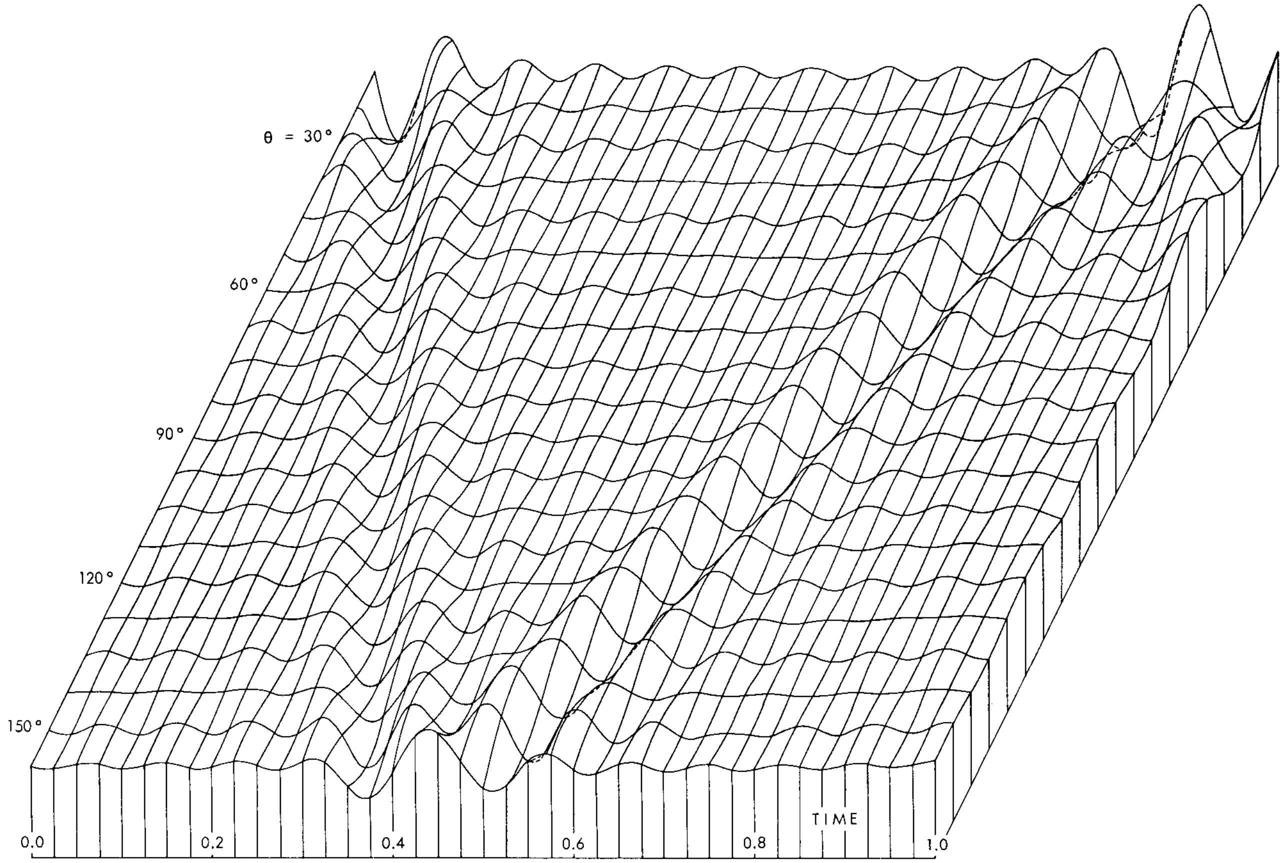

Figure 5 **Three-dimensional Figure of** $({}_1w_{10})$.